S. Lee and C. T.-C. Nguyen, "Mechanically-coupled micromechanical arrays for improved phase noise," *Proceedings*, IEEE Int. Ultrasonics, Ferroelectrics, and Frequency Control 50th Anniv. Joint Conf., Montreal, Canada, Aug. 24-27, 2004, pp. 280-286.

Mechanically-Coupled Micromechanical Resonator Arrays for Improved Phase Noise

Seungbae Lee and Clark T.-C. Nguyen

Center for Wireless Integrated Microsystems(WIMS)
Department of Electrical Engineering and Computer Science
University Of Michigan Ann Arbor, Michigan 48109-2122, U.S.A.
Tel.:(734)764-3352, Fax:(734)647-1781, email:seungbae@umich.edu

***Abstract* — Reductions in phase noise by more than 26 dB have been obtained over previous micromechanical resonator oscillators by replacing the single resonator normally used in such oscillators with a mechanically-coupled array of them to effectively raise the power handling ability of the frequency selective tank by a factor equal to the number of resonators used in the array, and all with virtually no increase in volume or cost, given that all resonators are integrated onto a single die using batch processed MEMS technology. Specifically, a mechanically-coupled array of ten 15.4-MHz 40μmx10μmx2μm free-free beams embedded in a positive feedback loop with a single-ended to differential transimpedance sustaining amplifier achieves phase noises of -109 and -133 dBc/Hz at 1 kHz and far-from-carrier offset frequencies, respectively. When divided down to 10 MHz, these effectively correspond to -112 and -136 dBc/Hz, respectively, which represent more than 17 and 26 dB improvements over recently published work with clamped-clamped beam resonator oscillators.**

***Keywords* – phase noise, MEMS, power handling, micromechanical resonator, free-free beam, clamped-clamped beam.**

I. Introduction

With recently demonstrated Q's in the tens of thousands and frequency temperature dependencies as small as 18 ppm over the 0-70°C commercial temperature range [1], integrated circuit (IC)-compatible vibrating micromechanical resonators achieved via MEMS technology are becoming very attractive as on-chip frequency selecting elements for communications-grade oscillators and filters. In fact, a recently demonstrated oscillator referenced to an SOI-based vibrating micromechanical resonator has already satisfied the GSM specifications (-130 and -150dBc/Hz at 1kHz and far-from-carrier offsets, respectively, from a 13MHz carrier) for communication reference oscillators [2]. In addition, a 60-MHz oscillator that combines a capacitively-transduced surface-micromachined wine-glass disk resonator [3] with a custom IC sustaining amplifier very nearly makes the GSM specification, achieving -125 and -147dBc/Hz at 1kHz and far-from-carrier offsets, respectively, when divided down to 10MHz. Of the two micromechanical oscillators, the surface-micromachined one is arguably the more attractive from an integration standpoint, since surface-micromachined MEMS devices have a more successful planar integration history [4]-[7]. Thus, it would be desirable to attain the GSM specification (and better for other applications) using surface-micromachined devices.

With a recognition that differences in power handling between bulk (i.e., SOI) and surface-micromachined devices are largely responsible for phase noise performance differences in oscillators referenced to them, this work investigates the use of mechanically coupled resonator arrays [8] to raise the power handling of surface-micromachined resonators and thereby allow substantial performance improvements when used in oscillator circuits. In particular, a mechanically-coupled array of ten 15.4-MHz 40μmx10μmx2μm free-free beams ("FF-beams") embedded in a positive feedback loop with a single-ended to differential transimpedance sustaining amplifier is demonstrated with phase noise densities of -109 and -133dBc/Hz at 1kHz and far-from-carrier offset frequencies, respectively. When divided down to 10-MHz, these effectively correspond to -112 and -136dBc/Hz, respectively, which represent more than 17 and 26dB improvements over recently published work using clamped-clamped beam resonators in oscillators [9].

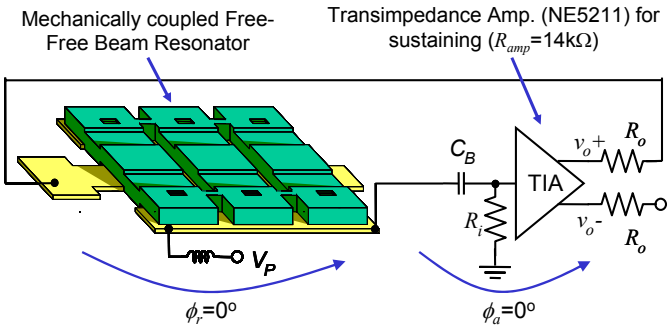

Fig. 1: Schematic of the series oscillator with transimpedance sustaining amplifier utilizing a mechanically-coupled free-free beam resonator array.

The demonstrated technique not only encourages a similar design approach for more GSM-capable resonator types (e.g., wine-glass disks), but also sheds light on the origins of the $1/f^3$ noise component commonly seen in micromechanical resonator oscillators farther from the carrier than in quartz crystal oscillators. In particular, mechanically-coupled arraying of resonators in this work has for the first time revealed the transition corner between $1/f^3$ and $1/f^2$ phase noise in a micromechanical resonator oscillator, suggesting that the troublesome $1/f^3$ noise indeed derives from resonator capacitive transducer nonlinearities generated by large vibration amplitude operation, as suggested by [10][11].

II. Basic Oscillator Design and Performance

Like previous off-chip oscillators design by the authors [11][12], the oscillator of this work uses a series resonant topology, shown in Fig. 1, in which the micromechanical frequency-setting device (depicted by a resonator array in Fig. 1) is embedded in a positive feedback loop together with an off-chip NE5211 transresistance sustaining amplifier possessing sufficient gain to initiate and sustain oscillation. Other than the use of a more advanced micromechanical resonator, the criteria governing start-up and sustenance of oscillation are identical to those described in [12]:

1. For Start-Up: $R_{amp} > R_x + R_i + R_o$
2. In Steady-State: $R_{amp} = R_x + R_i + R_o$
3. Loop Phase: 0^o around the positive feedback loop

where R_{amp}, R_i, and R_o are the gain, input resistance, and output resistance, of the transresistance sustaining amplifier, respectively; and R_x is the series motional resistance of mechanical resonator. In the series resonant circuit topology of Fig. 1, both the resonator (in resonance vibration) and the sustaining amplifier ideally sustain 0^o phase shifts across their terminals, resulting in a total loop phase shift of 0^o that satisfies criterion 3 above. By allowing the simple choice of its positive output terminal, the differential output stage of the NE5211 transresistance amplifier provides a 0^o phase shift without the need for a second amplifier stage—a feature that greatly extends the gain-bandwidth product of this circuit.

Like the work of [11] and [12], this oscillator limits when the series resistance R_x of its frequency setting micromechanical resonator (or resonator array) increases with amplitude to the point of satisfying criterion 2 above, after which steady-state oscillation ensues. In steady-state, the phase noise at small frequency offsets around the carrier frequency can be described by the expression

$$L\{f_m\} = \frac{2kTF}{P_o}\left[1+\left(\frac{f_o}{2Q\cdot f_m}\right)^2\right]+\left[K_1+K_2\cdot X_o^4\right]\cdot\frac{K_3}{f_m}\left(\frac{f_o}{f_m}\right)^2 \qquad (1)$$

where f_m is the offset from the carrier f_o at which phase noise is being evaluated; k is Boltzmann's constant; T is temperature in Kelvin; F is the noise factor of the sustaining amplifier [4]; P_o is the oscillator loop output power; K_1 and K_2 are resonator device dependent constants; K_3 is a $1/f$ noise constant, normally generated by the electronics; and X_o is the resonator amplitude of vibration. (1) is basically Leeson's expression [13], modified to account for nonlinear mixed $1/f$ noise aliased into the tank passband to generate $1/f^3$ close-to-carrier phase noise. In past work, it is this $1/f^3$ phase noise that has prevented oscillators referenced to surface-micromachined capacitively-driven resonators from attaining theoretically predicted close-to-carrier phase noise values, thereby preventing them from truly satisfying GSM specifications.

If the assumption in (1) that the $1/f^3$ noise arises from aliased $1/f$ noise is correct, then according to (1), the $1/f^3$ noise can be suppressed relative to the other noise dependencies (e.g., $1/f^2$) by reducing the resonator displacement X_o required to achieve a given power P_o in the oscillator loop. In other words, by raising the power handling capability of the frequency-setting resonator element, the $1/f^3$ noise term is predicted by (1) to shrink to a point where it is below the $1/f^2$ noise at offset frequencies far enough from the carrier, at which point the oscillator phase noise plot will be similar to that of quartz crystal oscillators, where both noise $1/f^3$ and $1/f^2$ dependencies are normally visible.

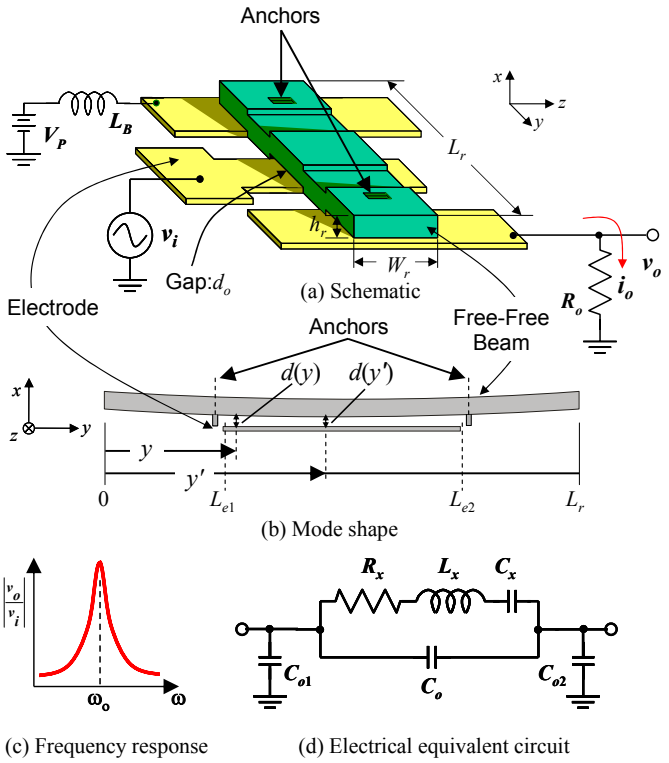

Fig. 2: (a) Perspective-view schematic of a one-port single free-free beam micromechanical resonator under a preferred bias and excitation scheme, (b) its mode shape, (c) example frequency response, and (d) equivalent electrical circuit.

As already mentioned in Section I, this work attempts to improve oscillator phase noise performance according to (1) by increasing the overall power handling ability of the resonator element via use of a mechanically-coupled array of resonators. The next two sections now focus on the array methodology.

III. Stud-Supported Free-Free Beam Resonator

Fig. 2 presents the perspective-view schematic of the one-port free-free beam ("FF-beam") vibrating micromechanical resonator used as the array element in this work, along with its mode shape, its *LCR* equivalent circuit, labels identifying key features, and a bias/excitation configuration suitable for use in a series oscillator topology. This device differs from a previously published version [14] in that it dispenses with torsional nodal supports, and rather uses anchoring studs directly at the beam's free-free mode nodal points. The fabrication process

TABLE I: STUD-SUPPORTED SINGLE FREE-FREE BEAM DESIGN

Parameter	Value	Units
Young's Modulus of PolySi, E	150	GPa
Density of PolySi, ρ	2,300	kg/m^3
μRes. Beam Thickness, h_r	2	μm
μRes. Beam Length, L_r	40	μm
μRes. Beam Width, W_r	10	μm
Electrode Width, W_e	16	μm
μRes. Beam Anchor Length, L_a	2	μm
μRes. Beam Anchor Width, W_a	1	μm
Electrode-to-μRes. Gap, d_o	3,000	Å
DC-bias, V_P	30	V
Resonator Mass @ I/O, m_r	1.25x10^{-12}	Kg
Resonator Stiffness @ I/O, k_r	11,690	N/m
Calc. Equiv. Inductance, L_x	8.48	H
Calc. Equiv. Resistance, R_x	121	kΩ
Calc. Equiv. Capacitance, C_x	0.0126	fF
Static Overlap Capacitance, C_o	4.7	fF
Parasitic In/Out Cap. $C_{o1} \approx C_{o2}$	250	fF
Meas. Quality Factor, Q	6,800	—
Meas. Center Frequency, f_o	15.4	MHz
Meas. Series Resistance, R_x	125	kΩ

used to achieve such anchoring studs is similar to that used for previous self-aligned disk resonators [15], except for a chemical mechanical polishing (CMP) step at the very end that greatly facilitates removal of sidewall stringers at the end of the process. The process sequence is summarized in the caption of Fig. 3(a)-(c), which presents cross-sections at several points in the process flow, culminating in the SEM of a stand-alone, stud-supported free-free beam micromechanical resonator in Fig. 3(d) to match the schematic of Fig. 2.

The design for resonance frequency and motional elements for this device are similar to that of previous torsional-beam-supported ones, so has been described earlier in [14], which contains all the needed design equations. Under normal operation using the excitation scheme of Fig. 2, a dc-bias voltage V_P is applied to the resonator structure, an ac signal v_i to the underlying electrode, and together these voltages generate an electrostatic drive force F_i, given by

$$F_i = V_P \frac{\partial C}{\partial x} V_i \qquad (2)$$

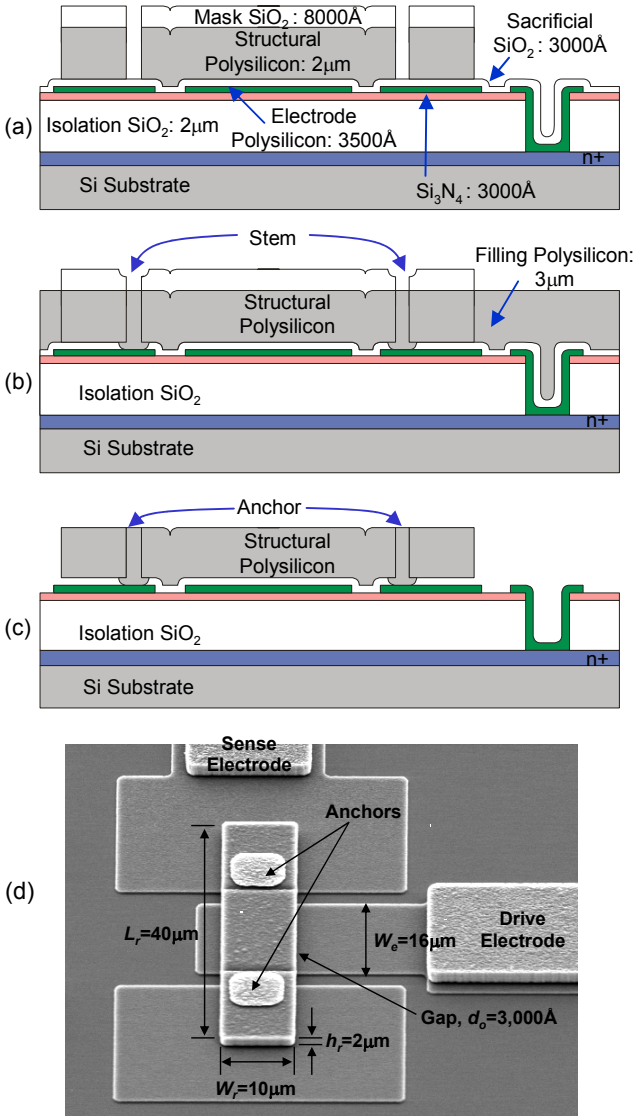

Fig. 3: Simplified self-aligned process flow for mechanically coupled micromechanical resonator array fabrication: (a) define ground plane, electrode, gap by sacrificial oxide, and structural device, (b) etch anchor openings, fill anchors with polysilicon, following with CMP and timed etch, (c) etch filling polysilicon with anchor protection, and release device by wet etch, and (d) an SEM of a fabricated device.

where V_i is the phasor input voltage, and $\partial C/\partial x$ is the integrated change in electrode-to-resonator overlap capacitance per unit displacement, given by (referring to Fig. 2(b))

$$\frac{\partial C}{\partial x} = \sqrt{\int_{L_{e1}}^{L_{e2}} \int_{L_{e1}}^{L_{e2}} \frac{(\varepsilon_o W_r)^2}{[d(y')d(y)]^2} \frac{k_{re}}{k_r(y')} \frac{X_m(y)}{X_m(y')} dy'dy} \qquad (3)$$

where $k_r(y)$ is stiffness as a function of beam location y, k_{re} is the effective lumped stiffness at the beam location centered over the electrode, $d(y)$ is the electrode-to-resonator gap spacing as a function of y, L_{e1} and L_{e2} are the y locations of the left and right edges of the electrode, and X_m is a function describing the vibration mode shape [14].

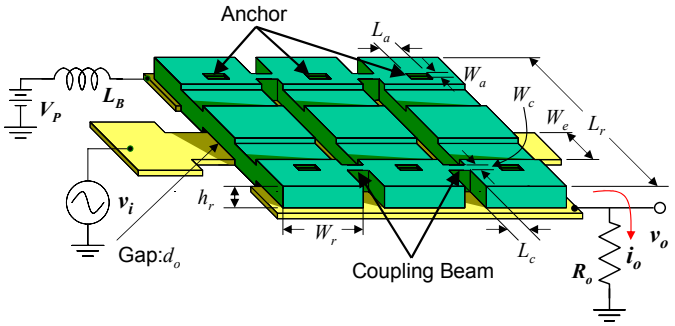

Fig. 4: Perspective-view schematic of a multi (three) free-free beam micromechanical resonator array.

The force F_i drives the beam into resonance vibration when the frequency of v_i matches the beam's free-free resonance frequency (c.f., Table I). Once vibrating, the ensuing dc-biased time-varying electrode-to-resonator capacitance generates an output current i_o given by

$$i_o = V_P \frac{\partial C}{\partial x}\frac{\partial x}{\partial t} = \omega_o \frac{Q}{k_{re}}\left(\frac{\partial C}{\partial x}\right)^2 V_P^2 v_i \qquad (4)$$

The maximum power that a single free-free beam can handle while still avoiding deleterious effects caused by nonlinearity can be expressed by

$$P_{o\max,1} = \omega_o \frac{k_{re}}{Q}(ad_o)^2 \qquad (5)$$

where a is the fraction of the electrode-to-resonator gap beyond which the onset of strong nonlinearities ensue, and the 1 indicates the expression corresponds to a single resonator. For the design of this work (summarized in Table I), with V_P=30V, and assuming a=0.4 the maximum power that a single free-free beam resonator can handle while retaining acceptable linearity is only 2.4μW. This is substantially smaller than the couple of milliwatts typically exhibited by larger quartz crystal resonators [16].

IV. Power-Handling Increases via Mechanically-Coupled Micromechanical Resonator Arrays

To increase the power handling ability of the vibrating micromechanical frequency setting element at a given maximum amplitude ad_o, this work harnesses the mechanically-coupled array concept of [8] to construct the structure of Fig. 4. Here, three (or more) free-free beam resonators, each identically designed to the specifications of Fig. 2 and Table I, are coupled mechanically by short torsional links connecting each adjacent resonator to one another at their torsional anti-nodes (which happen to be the same locations as the flexural nodal points). As described in [8], this mechanical connection of resonators actually realizes a multi-pole filter structure [17], that now has several modes of vibration (one mode for each resonator in the array). Each modal peak corresponds to a state where all resonators are vibrating at exactly the same frequency (i.e., at the frequency of the mode)—a feat accomplished by simple mechanical coupling that would be very difficult to achieve via frequency matching feedback electronics.

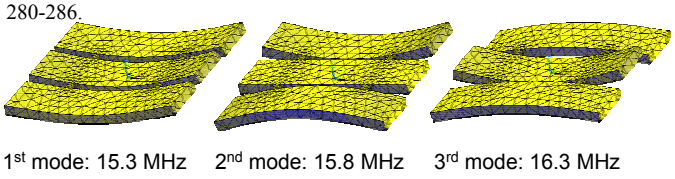

Fig. 5: ANSYS simulated mode shapes for mechanically coupled three free-free beam micromechanical resonator array.

Table II: Device Parameter Changes in a Mechanically Coupled n Resonator Array

Parameter	m_r	k_r	L_x	R_x	C_x	C_o
Change factor	n	n	$1/n$	$Q_1/(n*Q_n)$	n	n

The different modes of this structure are distinguished by the phasings between the resonators, as shown in Fig. 5. Here, in its first mode, the structure of Fig. 4 vibrates in a fashion where all of its constituent resonators are in phase. In its second mode, the center resonator stays still, while the resonators flanking it vibrate with opposite phasings. Finally, in its third mode, all resonators vibrate with phasings opposite the adjacent resonator.

Because each mode can be distinguished by its phasings, a single mode can be selected, with all others suppressed, by merely phasing the input ac signal to match the phasing of the desired mode. In this work, the first mode of the array is selected (with all other modes rejected) by merely using a single uniform input electrode under the midpoint of all resonators. This electrode choice accentuates the first mode, where all resonators vibrate in phase, while suppressing the other modes, where some resonators vibrate with opposing phasings. If one of the other modes is desired, a combination of electrodes where some of them are under the beam midpoints, and some under the beam outer edges, can be chosen to accentuate the appropriate mode. It should be noted that the use of stiff torsional couplers attached at the torsional anti-nodes of each device serves to spread the modal peaks of the filter structure in Fig. 4 far apart [18], which facilitates the selection of one, and only one, of the peaks.

Once a single mode is selected via proper electrode placement, the structure practically behaves as a single resonator, but with a current handling ability equal to the sum of the currents from all constituent resonators. Thus, the power handling expression for a mechanically coupled array can be expressed as

$$P_{o\max,n} = \omega_o \frac{k_{rn}}{Q_n}(ad_o)^2 = \omega_o \frac{n \cdot k_{re}}{Q_n}(ad_o)^2 \qquad (6)$$

where n is the number of resonators in the array; and k_{rn} and Q_n are the stiffness and quality factor of the resonator array, respectively. (6) indicates that the array can handle a larger

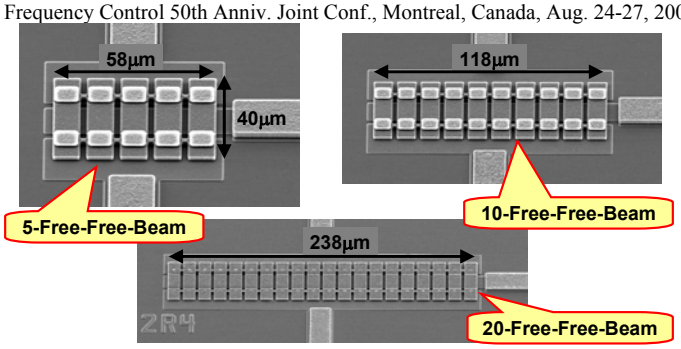

Fig. 6: Scanning Electron Micrographs (SEM) of mechanically coupled micromechanical resonator arrays with varying number of free-free beams coupled.

amount of power than a single resonator by a factor of $n*Q_1/Q_n$, where Q_1 is the quality factor of single resonator. At the same time, the series motional resistance of the array also decreases by a factor of $n*Q_n/Q_1$. Table II indicates the factors by which the various parameters in Table I change when n resonators are arrayed as in Fig. 4.

In effect, the power handling increase afforded by arraying amounts to the same thing as increasing the electrode-to-resonator area of a given resonator design by n times, with perhaps less Q degradation and smaller frequency deviations. It should be noted that in the present work a similar area increase could have also been attained by merely increasing the width of a single free-free beam, rather than arraying many smaller ones. One advantage, however, of a resonator beam array is that the anchor losses of such a structure can be much smaller than that of a wider beam structure, especially if the selected cumulative mode is one where resonators are moving out-of-phase, and thus, canceling energy losses to the substrate. The advantages of a mechanically-coupled resonator array are perhaps most apparent when applied to lateral resonators, where area increases in a single resonator are much more difficult to realize.

V. Experimental Results

Stand-alone free-free beam resonators (as depicted in Fig. 2) and mechanically-coupled arrays of them using 5, 10, and 20 resonators, were fabricated using the self-aligned anchor-stud process flow described in Fig. 3. Each array design utilizes identical constituent resonators with designs summarized in Table I, and with coupling beams identically dimensioned to be 2 μm-long, 1.6 μm-wide, and 2 μm-thick. Fig. 6 presents SEM's of each mechanically coupled micromechanical resonator array.

Before actual oscillator testing, stand-alone FF-beams and mechanically coupled arrays of them were first tested to verify the device theory of Sections III and IV. For testing, a custom-built vacuum chamber into which a board and casing housing resonators and oscillators could be inserted, was used together with a turbomolecular pump capable of pumping the chamber down to pressures as low as 4 μTorr. The vacuum chamber includes electrical feedthroughs that allow interconnections to

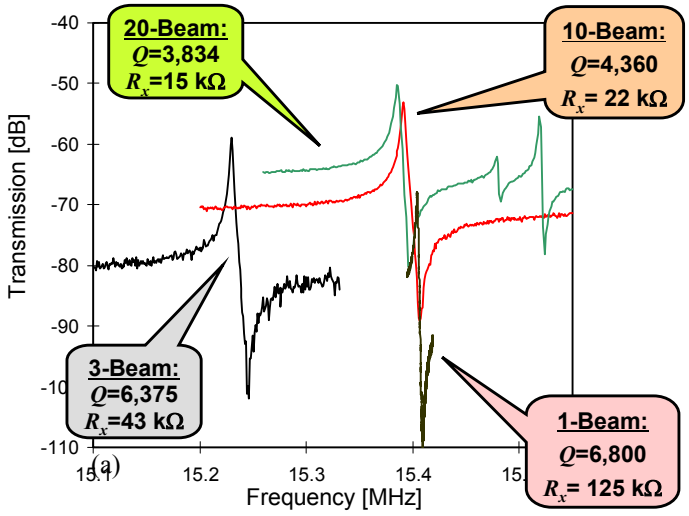

Fig. 7: Frequency spectra of open loop test for mechanically-coupled free-free beam array with measurement condition: V_i = 71mV, V_P =30V, in 40 mTorr vacuum.

external measurement instrumentation—in this case, an HP8751A Network Analyzer used to obtain frequency characteristics for the devices in question.

A. Mechanically-Coupled Resonator Arrays

Fig. 7 presents measured frequency spectra for a stand-alone FF-beam together with those for fabricated FF-beam resonator arrays with three, ten, and twenty free-free beams mechanically coupled with one another. Each measurement was taken under identical excitation conditions, with V_P=30V and V_i=71mV. As advertised, the arrays exhibit lower series motional resistances R_x than the single resonator, lowering its effective value from 125kΩ for the single resonator, to 15kΩ for the 20 resonator array—an overall reduction by about 8.3X. The observed reductions in series resistance R_x are not equal to the number of resonators used in each array, as was the case in [8], mainly because the Q of the larger FF-beam resonator arrays in this work suffered more from anchor losses, given that they possessed a larger total number of anchors. The R_x reductions, however, are consistent with the expected factors $n*Q_n/Q_1$=2.8, 6.4, and 11.4, for the 3, 10, and 20, resonator arrays, respectively. Note that even the lowest Q of 3,834 for the 20 resonator array is still sufficient to attain a good performing reference oscillator.

B. Series Resonant Micromechanical Resonator Oscillator

Pursuant to evaluating oscillators utilizing the above resonator array variants, off-chip NE5211 transimpedance amplifiers were mounted together with resonator die onto pc boards, on which they were interconnected electrically via wire-bonding. The pc boards were enclosed in aluminum boxes for ground stability, then inserted into the custom-built vacuum chamber for testing under a 40 mTorr vacuum.

Fig. 8 compares plots of phase noise density versus frequency offset for the 15.4-MHz, ten mechanically-coupled free-free beam array oscillator operating at various output am-

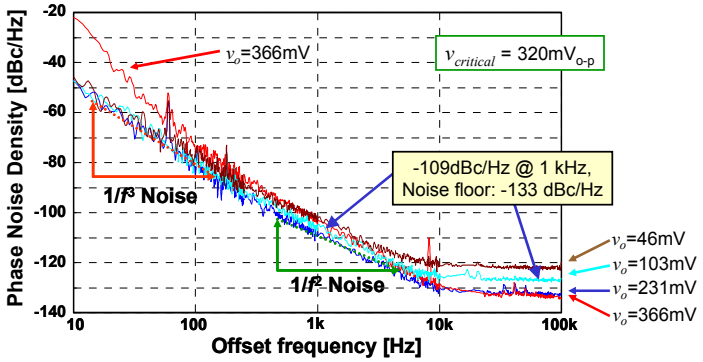

Fig. 8: Measured phase noise density-to-carrier power ratio versus carrier offset frequency for the micromechanical resonator oscillator using ten free-free coupled beam array.

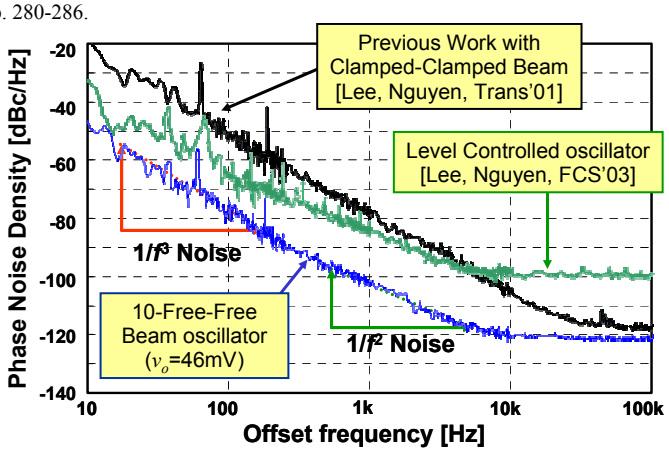

Fig. 9: Phase noise performance comparison of the 10-FF-beam mechanically-coupled array oscillator with previous clamped-clamped beam micromechanical oscillators.

plitudes, with each measured under 40 mTorr vacuum using an HPE5500 Phase Noise Measurement System. As expected, the far-from-carrier phase noise is directly dependent on oscillation (i.e., vibration) amplitude, improving as the oscillation amplitude (i.e., output power) increases, as predicted by (1). At offset frequencies just below 10kHz, phase noise with a $1/f^2$ frequency dependence is seen for the first time in a non-automatic-level-controlled surface-micromachined resonator oscillator, verifying the prediction of (1) that higher power through the resonator places the oscillator in a regime where $1/f^2$ noise dominates over $1/f^3$. At carrier offsets below 100Hz, $1/f^3$ dominates. Interestingly, for all oscillation amplitudes except the largest, the phase noise density seems to equalize in this offset frequency regime, suggesting that the $1/f^3$ component is largely independent of the oscillation amplitude. This further indicates that there is a threshold vibration amplitude where resonator behavior abruptly transitions from a relatively linear state to a nonlinear one, and then holds this degree of nonlinearity over a range of large amplitudes. When the amplitude exceeds the critical Duffing value (in this case, when v_i >320mV), the phase noise at close-to-carrier offsets experiences a sudden increase, which is thought to arise due to the hysteretic instability that occurs when vibration amplitudes exceed the critical Duffing point [11][12].

The best overall phase noise performance is achieved when the oscillation amplitude is v_i =231mV, which is just below the critical Duffing value. At this oscillation amplitude, the 15.4-MHz oscillator achieves phase noise densities of -109 and -133 dBc/Hz at 1kHz and far-from-carrier offset frequencies, respectively. When divided down to 10-MHz, these effectively correspond to -112 and -136dBc/Hz, respectively, which represent more than 17 and 26dB improvements over recently published work using a clamped-clamped beam micromechanical resonator as the frequency setting element of a similar oscillator [9].

Fig. 9 directly compares the performance of the oscillators of this work with those of previous versions using "beam-type" resonators (running under approximately the same output power level, where possible). Here, the phase noise performance of the oscillator using the 10-FF-beam mechanically-coupled array is clearly much better than that of those using the single CC-beam resonator. The improved performance derives from (1) the higher Q of the arrays, which suffers much less from anchor dissipation than a CC-beam due to the use of FF-beams in their structure; and (2) the larger power handling ability of the array, which leads to a smaller $1/f^3$ component. As predicted by (1), higher Q effectively pushes the noise corner (where white phase noise meets non-white phase noise) closer to the carrier, and this is especially visible when comparing the non-automatic-level-controlled (non-ALC'ed) oscillators of Fig. 9. Note that although automatic-level-control (ALC) completely removes the $1/f^3$ phase noise of the CC-beam oscillator, as found in [12], it does so at the expense of oscillation amplitude, which substantially degrades its far-from-carrier phase noise density. This then leaves the ALC'ed oscillator with much worse phase noise at both close- and far-from-carrier offsets than that of the oscillators using non-ALC'ed mechanically-coupled resonator arrays.

VI. Conclusions

The use of a mechanically-coupled array to multiply the power handling ability of a micromechanical frequency-setting element to a value several times that of a single of its constituent micromechanical resonators has been demonstrated to greatly reduce the close- and far-from-carrier phase noise density of an oscillator reference to this structure. In particular, a 15.4-MHz series resonant oscillator referenced to a mechanically-coupled array of 10 free-free-beam micromechanical resonators was demonstrated with an effective phase noise density, when divided down to 10 MHz, more than 17 dB and 26 dB better at 1kHz and far-from-carrier offsets, respectively, than that of a recently published oscillator using a single clamped-clamped beam resonator. Much of the improvement in the phase noise performance of this oscillator derives from not only reductions in far-from-carrier noise, but also close-to-carrier $1/f^3$ phase noise—the same $1/f^3$ phase noise that has plagued many previous capacitively-transduced micromechanical resonator oscillators, preventing them from meeting

S. Lee and C. T.-C. Nguyen, "Mechanically-coupled micromechanical arrays for improved phase noise," *Proceedings*, IEEE Int. Ultrasonics, Ferroelectrics, and Frequency Control 50th Anniv. Joint Conf., Montreal, Canada, Aug. 24-27, 2004, pp. 280-286.

GSM reference oscillator specifications. That this $1/f^3$ phase noise component can be suppressed by reducing the resonator vibration amplitude required to pass the needed oscillator power verifies the hypothesis of [10] that this noise component does indeed derive from $1/f$ noise aliased into the oscillator passband by the transducer nonlinearity of the mechanical resonator.

Due to its use of free-free beam micromechanical resonators, this work did not yield an oscillator that satisfies the GSM cellular telephone reference oscillator phase noise specification. However, it now encourages application of the same mechanically-coupled arraying technique to much more appropriate wine-glass disk resonators, which have already been used in oscillators that very nearly make the GSM specification [3]. Work towards a wine-glass array oscillator is already in progress.

ACKNOWLEDGMENT

This work was supported under DARPA Cooperative Agmt. No. F30602-01-1-0573.

REFERENCES

[1] W. -T. Hsu and C. T.-C. Nguyen, "Stiffness-compensated temperature-insensitive micromechanical resonators," *Technical Digest*, 2002 IEEE Int. Micro Electro Mechanical Systems Conf., Jan. 20-24, 2002, pp. 731-734.

[2] V. Kaajakari, T. Mattila, A. Oja, J. Kiihamäki, and, H. Seppä, "Square-extensional mode single-crystal silicon micromechanical resonator for low phase noise oscillator applications," *IEEE Electron Device Letters*, vol. 25, no. 4, pp. 173-175, April 2004.

[3] Y. Lin; S. Lee; S. Li; Y. Xie; Z. Ren; and C. T.-C. Nguyen; "60-MHz Wine-Glass Micromechanical-Disk Reference Oscillator," *Digest of Technical Papers*, 2004 IEEE International Solid-State Circuits Conference, San Francisco, CA, Feb. 15-19, 2004, pp. 322 – 331

[4] C. T.-C. Nguyen and R. T. Howe, "An integrated CMOS micromechanical resonator high-*Q* oscillator," *IEEE J. Solid-State Circuits*, vol. 34, no. 4, pp. 440-455, April 1999.

[5] T. A. Core, W. K. Tsang, S. J. Sherman, "Fabrication technology for an integrated surface-micromachined sensor," *Solid State Technology*, pp. 39-47, Oct. 1993.

[6] A. E. Franke, D. Bilic, D. T. Chang, P. T. Jones, T.-J. King, R. T. Howe, and G. C. Johnson, "Post-CMOS integration of germanium microstructures," *Tech. Digest*, 12th Int. IEEE MEMS Conf., Orlando, Florida, Jan. 17-21, 1999, pp. 630-637.

[7] A.-C. Wong, Y. Xie, and C. T.-C. Nguyen, "A bonded-micro-platform technology for modular merging of RF MEMS and transistor circuits," *Dig. of Tech. Papers*, Transducers'01, Munich, Germany, June 10-14, 2001, pp. 992-995.

[8] M. Demirci and C. T.-C. Nguyen, "Mechanically corner-coupled square microresonator array for reduces series motional resistance," *Digest of Technical Papers*, the 12th Int. Conf. on Solid-State Sensors & Actuators (Transducers'03), Boston, MA, June 8-12, 2003, pp.955-958

[9] Y. Lin, S. Lee, Z. Ren, and C. T.-C. Nguyen, "Series resonant micromechanical resonator oscillator," *Technical Digest*, IEEE Int. Electron Devices Conf. (IEDM'03), Washington D.C., December 7-10, 2003, pp. 431-434.

[10] S. Lee, M. U. Demirci, and C. T.-C. Nguyen, "A 10-MHz micromechanical resonator Pierce reference oscillator for communications," *Digest of Technical Papers*, the 11th Int. Conf. on Solid-State Sensors & Actuators (Transducers'01), Munich, Germany, June 10-14, 2001, pp. 1094-1097.

[11] S. Lee and C. T.-C. Nguyen, "Phase noise amplitude dependence in self-limiting wine-glass disk oscillators," *Technical Digest,* Solid-State Sensor, Actuator and Microsystems Workshop (HiltonHead'04), Hilton Head Island, South Carolina, June 6-10, 2004, pp.33-36.

[12] S. Lee and C. T.-C. Nguyen, "Influence of automatic level control on micromechanical resonator oscillator phase noise," *Proceedings of 2003 IEEE Frequency Control Symposium*, Tampa, Florida, May 5-8, 2003, pp.341-349.

[13] D. B. Leeson, "A simple model of feedback oscillator noise spectrum," *Proc. IEEE*, vol. 54, pp. 329-330, Feb. 1966.

[14] K. Wang, A. Wong, and C. T.-C. Nguyen, "VHF free-free beam high-*Q* micromechanical resonators," *Journal of MEMS*, vol.9, No.3, pp.347-360, September 2000.

[15] J. Wang, Z. Ren, and C. T.-C. Nguyen, "Self-aligned 1.14-GHz vibrating radial-mode disk resonators," *Digest of Technical Papers*, the 12th Int. Conf. on Solid-State Sensors & Actuators (Transducers'03), Boston, Massachusetts, June 8-12, 2003, pp. 947-950.

[16] R. J. Matthys, *Crystal Oscillator Circuits*. New York: Wiley, 1983.

[17] K. Wang, and C. T.-C. Nguyen, "High-order medium frequency micromechanical electronic filters," *Journal of MEMS*, vol.8, No.4, pp.534-557, December 1999.

[18] F. D. Bannon III, J. R. Clark, and C. T.-C. Nguyen, "High frequency micromechanical filters," *IEEE J. Solid-State Circuits*, vol. 35, no. 4, pp. 512-526, April 2000.